Fe₃O₄@SiO₂–MoO₃H nanoparticles: a magnetically recyclable nanocatalyst system for the synthesis of 1,8-dioxo-decahydroacridine derivatives†

Mahtab Kiani*[a] and Mohammad Mohammadipour[b]

Molybdic acid-functionalized silica-coated nano-Fe₃O₄ particles (Fe₃O₄@SiO₂–MoO₃H) have been prepared as a novel heterogeneous acid catalyst using a facile process. The material was subsequently identified as an efficient catalyst for the synthesis of 1,8-dioxo-decahydroacridine derivatives under solvent free conditions. The catalyst could be readily recovered using a simple external magnet and reused several times without any significant loss in activity. Short reaction time, excellent yields and simple work-up are the advantages of this procedure.

Introduction

Nanocatalysis is a rapidly growing field which involves the use of nanomaterials as catalysts for a variety of homogeneous and heterogeneous catalysis applications.[1–3]

Magnetic nanoparticles (MNPs) have attracted growing interest in biomedical applications such as targeted drug delivery, magnetic resonance contrast, therapeutic agents, labeling and sorting of cells and bioseparation.[4,5]

Fe₃O₄ is a very popular magnetic media type absorber due to its unique magnetic features, low-cost and strong absorption characteristics.[6] However, pure Fe₃O₄ materials usually suffer from ease of oxidation, fast heat transfer and poor flame-retardant effect, which limit their applications. To solve these problems, various inorganic and polymeric materials have been reported as carriers of magnetic materials.[7] Among them, the silica coating is a very good surface modifier, because of its excellent stability, biocompatibility, nontoxicity and easily furthered conjugation with various functional groups, thus enabling the coupling and labeling of biotargets with selectivity and specificity.[8]

Magnetic hollow silica materials with different morphology and structure have been synthesized by the different methods.[9] The protective silica layer can minimize the aggregation of MNPs by reducing the magnetic dipolar attraction and provides a chemically inert surface to MNPs in biological environments. Furthermore, silica-coated MNPs can be easily activated to anchor various functional groups owing to abundant Si–OH groups on the silica surface. The fabrication of silica-coated MNPs with controlled magnetism require the simultaneous control of surface morphology and the thickness of nonmagnetic silica layer relative to the size of magnetic core.[10]

Acridine-1,8-dione derivatives as a class of interesting heterocyclic compounds exhibit numerous publications in organic, pharmaceutical and medicinal chemistry fields because of their potential biological activities and presence in a variety of significant natural products and synthetic dye-stuffs.[11] Acridine derivatives have been used as anti-tumor,[12] cytotoxic,[13] anti-fungal properties,[14] antimicrobial,[15] anti-cancer[16] and anti-multidrug-resistant.[17]

There are several methods reported in the literature for the synthesis of 1,8-dioxo-decahydroacridines *via* three component coupling of aldehydes, dimedone and amines in the presence of diverse catalysts including proline,[18] benzyltriethyl ammonium chloride (TEBAC),[19] fluorotailed acidic imidazolium salts,[20] 1-methylimidazolium trifluoroacetate [Hmim]TFA,[21] ceric ammonium nitrate (CAN),[22] silica-bonded *N*-propyl sulfamic acid (SBNPSA),[23] amberlyst-15,[24] carbon-based solid acid (SBSA),[25] and 4-dodecylbenzenesulfonic acid (DBSA).[26] However, many of these methods suffer from disadvantages such as low yields, toxic organic solvents, long reaction times, expensive catalysts, the requirement of special apparatus, laborious work-up procedures, and harsh reaction conditions. Thus, the development of simple, efficient, high-yielding and eco-friendly methods using new catalysts for the synthesis of these compounds would be highly desirable.

During the course of our recent research program on the development of new condition for organic transformations,[27–29] recently, molybdic acid-functionalized silica-coated nano-Fe₃O₄ particles have been prepared in our laboratory. It displayed a high stability and an impressive catalytic activity in the synthesis of 1,8-dioxo-decahydroacridine derivatives under solvent free conditions. The performance and recyclability behavior of this nano magnetic catalyst in the preparation of

[a]*Young Researchers and Elite Club, Karaj Branch, Islamic Azad University, Karaj, Iran. E-mail: mahtabkiani47@yahoo.com*

[b]*Department of Chemistry, Semnan University, Semnan 35131-19111, Iran*

1,8-dioxo-decahydroacridine is reported in this study to extend possibilities of this new catalyst.

Experimental

Methods and materials

The chemicals were purchased from Merck and Aldrich chemical companies. The reactions were monitored by TLC (silica-gel 60 F 254, hexane : EtOAc). Fourier transform infrared (FT-IR) spectroscopy spectra were recorded on a Shimadzu-470 spectrometer, using KBr pellets and the melting points were determined on a KRUSS model instrument. ^{1}H NMR spectra were recorded on a Bruker Avance II 400 NMR spectrometer at 400 MHz, in which DMSO-d_6 was used as solvent and TMS as the internal standard. X-ray diffraction (XRD) pattern was obtained by Philips X Pert Pro X diffractometer operated with a Ni filtered Cu Kα radiation source. Transmission electron microscopy (TEM) images of the electrocatalyst were recorded using a Philips CM-10 TEM microscope operated at 100 kV. Field emission scanning electron microscopy (SEM) and X-ray energy dispersive spectroscopy (EDS) analyses were carried out on a PHILIPS XL30, operated at a 20 kV accelerating voltage. Thermo gravimetric analyses (TGA) were conducted on a Rheometric Scientific Inc. 1998 thermal analysis apparatus under a N$_2$ atmosphere at a heating rate of 10 °C min^{-1}. The magnetic measurement was carried out in a vibrating sample magnetometer (Model 7407 VSM system, Lake Shore Cryotronic, Inc., Westerville, OH, USA) at room temperature. The inductively coupled plasma (ICP-OES) spectra were recorded using a Perkin-nElmer Optima 7300 DV series.

General procedure for the preparation of nano-Fe$_3$O$_4$ 1

FeCl$_3$·6H$_2$O (20 mmol) and FeCl$_2$·4H$_2$O (10 mmol) were dissolved in distilled water (100 ml) in a three-necked round-bottom flask (250 ml). The resulting transparent solution was heated at 90 °C with rapid mechanical stirring under N$_2$ atmosphere for 1 h. A solution of concentrated aqueous ammonia (10 ml, 25 wt%) was then added to the solution in a drop-wise manner over a 30 min period using a dropping funnel. The reaction mixture was then cooled to room temperature and the resulting magnetic particles collected with a magnet and rinsed thoroughly with distilled water.

General procedure for the preparation of nano-Fe$_3$O$_4$@SiO$_2$ 2

Nano-Fe$_3$O$_4$@SiO$_2$ was synthesized according to a previously published literature method. Magnetic nano particles (1.0 g) were initially diluted *via* the sequential addition of water (20 ml), ethanol (60 ml) and concentrated aqueous ammonia (1.5 ml, 28 wt%). The resulting dispersion was then homogenized by ultrasonic vibration in a water bath. A solution of TEOS (0.45 ml) in ethanol (10 ml) was then added to the dispersion in a drop-wise manner under continuous mechanical stirring. Following a 12 h period of stirring, the resulting product was collected by magnetic separation and washed three times with ethanol.

General procedure for the preparation of nano-Fe$_3$O$_4$@SiO$_2$–OMoO$_3$H 3

To an oven-dried (125 °C, vacuum) sample of nano-Fe$_3$O$_4$@SiO$_2$ (2 g) in a round bottomed flask (50 ml) equipped with a condenser and a drying tube, thionyl chloride (8 ml) was added and the mixture in the presence of CaCl$_2$ as a drying agent was refluxed for 48 h. The resulting dark powder was filtered and stored in a tightly capped bottle. To a mixture of Fe$_3$O$_4$@SiO$_2$–Cl (1 g) and sodium molybdate (0.84 g) *n*-hexane (5 ml) was added. The reaction mixture was stirred under refluxing conditions (70 °C) for 4 h. After completion of the reaction, the reaction mixture was filtered and washed with distilled water, and dried and then stirred in the presence of 0.1 N HCl (20 ml) for an hour. Finally, the mixture was filtered, washed with distilled water, and dried to afford nano-Fe$_3$O$_4$@SiO$_2$–OMoO$_3$H.

General procedure for the preparation of 1,8-dioxo-decahydroacridine derivatives 8

A mixture of 1,3-cyclohexanedione (2 mmol), aromatic aldehyde (1 mmol), ammonium acetate (1 mmol) and nano-Fe$_3$O$_4$@SiO$_2$–OMoO$_3$H (0.02 g) in a round bottom flask was heated with stirring in the oil bath at 100 °C for appropriate times. During the procedure, the reaction was monitored by Thin Layer Chromatography (TLC). The reaction mixture was cooled, eluted with hot ethanol (5 ml), and centrifuged to collect the catalyst. The solvent was evaporated with reduced pressure to collect the formed precipitate. The crude product was recrystallized from ethanol to yield pure 1,8-dioxo-decahydroacridines.

Spectral data

9-Phenyl-3,4,6,7,9,10-hexahydroacridine-1,8(2H,5H)-dione (7a). Mp: 278–279 °C; IR (KBr, cm^{-1}) ν: 3273, 3196, 3080, 1624, 1601, 1483, 1218, 1140. ^{1}H NMR (400 MHz, DMSO): δ 1.90–2.09 (m, 4H), 2.26–2.28 (m, 2H), 2.30–2.38 (m, 2H), 2.51–2.64 (m, 4H), 4.79 (s, 1H), 7.05–7.09 (t, J = 7.6, 2H), 7.11–7.12 (d, J = 8.4 Hz, 1H), 7.23–7.31 (dd, J = 8, 24.2, 2H), 9.17 (s, 1H). Anal. calc. for C$_{19}$H$_{19}$NO$_2$; C 77.79, H 6.53, N 4.77, O 10.91; found: C 77.73, H 6.59, N 4.71, O 10.92.

9-(4-Bromophenyl)-3,4,6,7,9,10-hexahydroacridine-1,8(2H,5H)-dione (7c). Mp: 311–312 °C; IR (KBr, cm^{-1}) ν: 3340, 3244, 2958, 2927, 1647, 1627, 1549, 1450, 1367, 1227, 1171. ^{1}H NMR (400 MHz, DMSO): δ 1.92–2.08 (m, 4H), 2.28–2.32 (m, 2H), 2.34–2.40 (m, 2H), 2.53–2.65 (m, 4H), 4.76 (s, 1H), 7.13–7.27 (m, 2H), 7.33–7.43 (dd, J = 30.6, 8.4 Hz, 2H), 9.38 (s, 1H). ^{13}C NMR (100 MHz, DMSO-d_6): δ 20.10, 20.27, 27.13, 31.39, 36.76, 36.90, 112.08, 117.66, 127.83, 129.43, 146.47, 151.59, 171.19, 194.58. Anal. calc. for C$_{19}$H$_{18}$BrNO$_2$; C 61.30, H 4.87, N 3.76, O 8.60; found: C 61.33, H 4.81, N 3.71, O 8.69.

9-(*p*-Tolyl)-3,4,6,7,9,10-hexahydroacridine-1,8(2H,5H)-dione (7d). Mp: 254–255 °C; IR (KBr, cm^{-1}) ν: 3286, 3203, 3068, 2943, 2887, 1639, 1608, 1458, 1364, 1232, 1176. ^{1}H NMR (400 MHz, DMSO): δ 1.96–2.07 (m, 4H), 2.26 (s, 3H), 2.29–2.42 (m, 4H), 2.52–2.69 (m, 4H), 4.79 (s, 1H), 7.03–7.05 (d, J = 8 Hz, 2H), 7.12–7.21 (d, J = 7.6 Hz, 2H), 9.18 (s, 1H). ^{13}C NMR (100 MHz, DMSO-d_6): δ 20.31, 21.06, 27.15, 31.22, 36.98, 55.14, 113.52, 117.03,
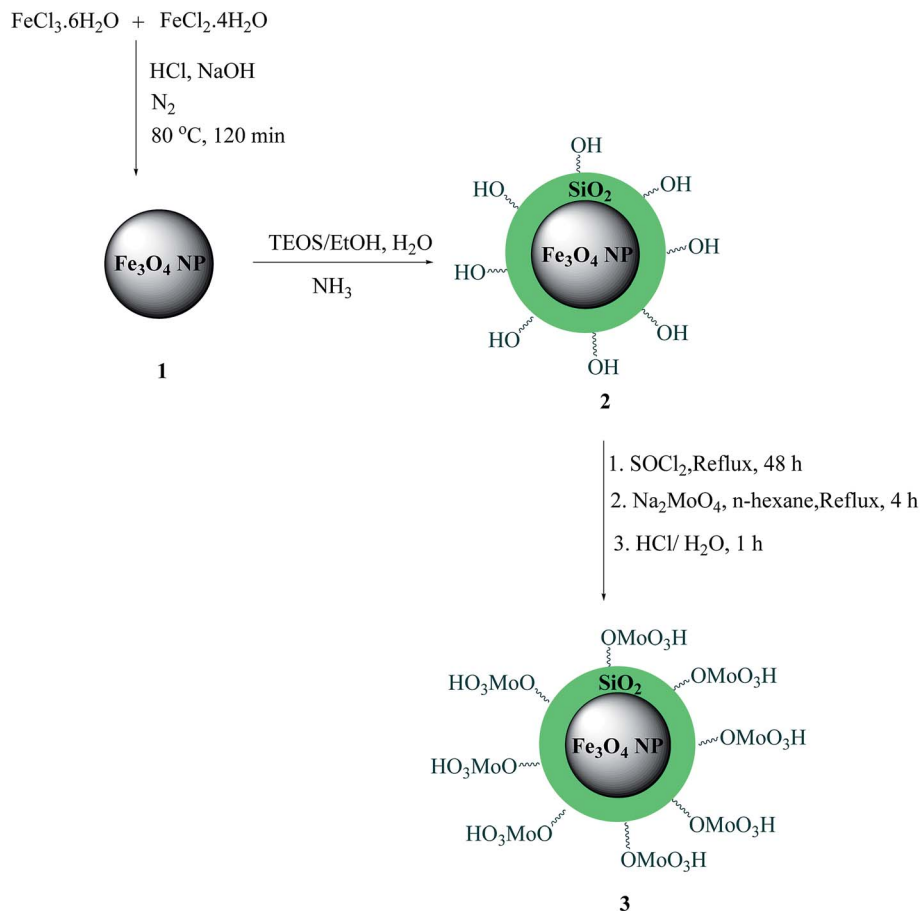
Scheme 1 Schematic of the procedure for the preparation of $Fe_3O_4@SiO_2-MoO_3H$.

128.25, 128.84, 129.33, 135.86, 146.36, 150.53, 169.57, 194.52. Anal. calc. for $C_{20}H_{21}NO_2$; C 78.15, H 6.89, N 4.56, O 10.41; found: C 78.19, H 6.83, N 4.58, O 10.45.

3,3,6,6-Tetra methyl-9-phenyl-3,4,6,7,9,10-hexahydroacridine-1,8-(2H,5H)-dione (8a). Mp: 191–193 °C; IR (KBr, cm^{-1}) ν: 3279, 3209, 3063, 2955, 2932, 1636, 1605, 1481, 1365, 1219, 1142. ^{1}H
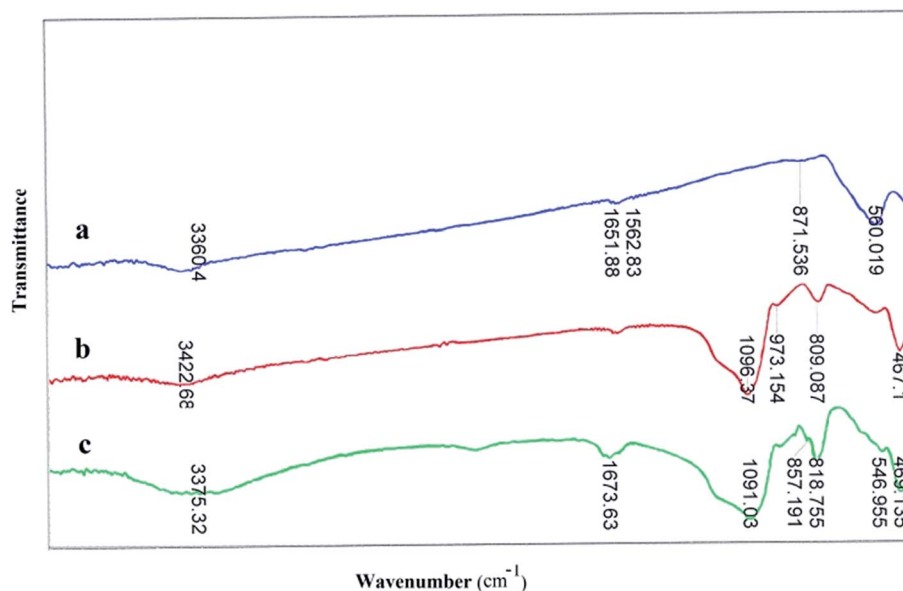

Fig. 1 The comparative FT-IR spectra of (a) Fe_3O_4 NPs (b) $Fe_3O_4@SiO_2$ and (c) $Fe_3O_4@SiO_2-OMoO_3H$.
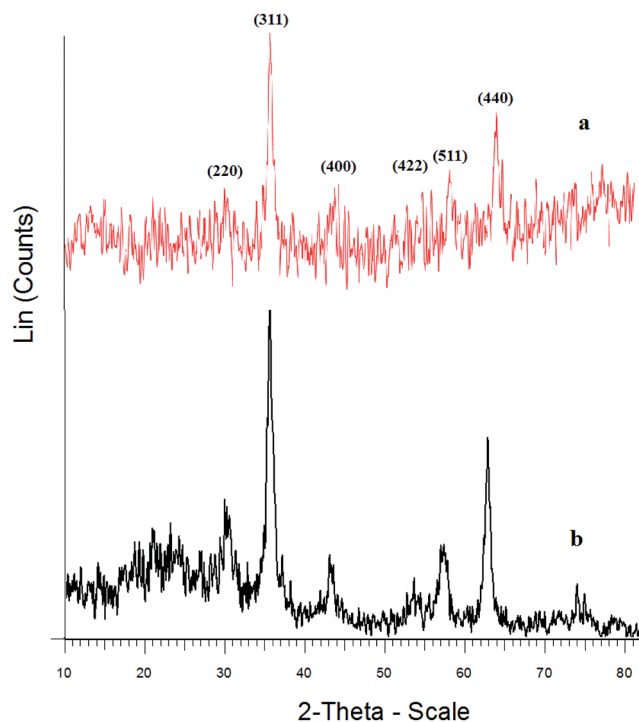
Fig. 2 X-ray powder diffraction patterns of (a) Fe₃O₄ NPs, (b) Fe₃-O₄@SiO₂–OMoO₃H.

NMR (400 MHz, DMSO): δ 0.84 (s, 6H), 0.99 (s, 6H), 1.96 (d, *J* = 21.5 Hz, 2H), 2.15 (d, *J* = 21.5 Hz, 2H), 2.30 (d, *J* = 22.8 Hz, 2H), 2.40–2.49 (m, 2H), 4.8 (s, 1H), 7.00–7.14 (m, 5H), 9.28 (s, 1H). ¹³C NMR

(100 MHz, DMSO-d₆): δ 26.45, 29.13, 32.14, 32.86, 50.24, 111.47, 125.46, 127.56, 127.63, 147.15, 149.32, 194.36. Anal. calc. for C₂₃H₂₇NO₂; C 79.05, H 7.79, N 4.01, O 9.16; found: C 79.08, H 7.73, N 4.06, O 9.11.

9-(4-Methoxyphenyl)-3,3,6,6-tetramethyl-3,4,6,7,9,10-hexahydroacridine-1,8(2H,5H)-dione (8b). Mp: 275–277 °C; IR (KBr, cm⁻¹) ν: 3277, 3203, 3070, 2959, 2870, 1643, 1606, 1508, 1483, 1367, 1223, 1171. ¹H NMR (500 MHz, DMSO): δ 0.90 (s, 6H), 1.04 (s, 6H), 2.08 (d, *J* = 9.7 Hz, 2H), 2.26 (d, *J* = 9.9 Hz, 2H), 2.48–2.52 (m, 2H), 2.57 (d, *J* = 10.8 Hz, 2H), 3.68 (s, 3H), 4.7 (s, 1H), 6.77–6.78 (t, *J* = 4.1, 2H), 7.06–7.08 (t. *J* = 5.12 Hz, 2H), 9.21 (s, 1H). Anal. calc. for C₂₄H₂₉NO₃; C 75.96, H 7.70, N 3.69, O 12.65; found: C 75.90, H 7.72, N 3.62, O 12.69.

9-(4-Fluorophenyl)-3,3,6,6-tetramethyl-3,4,6,7,9,10-hexahydroacridine-1,8(2H,5H)-dione (8e). Mp: 289–291 °C; FT-IR (KBr, cm⁻¹) ν: 3280, 3197, 3070, 2954, 2869, 1635, 1608, 1570, 1437, 1364, 1256, 1145. ¹H NMR (400 MHz, DMSO): δ 0.99 (s, 6H), 1.11 (s, 6H), 2.15–2.26 (dd, *J* = 28, 16 Hz, 4H), 2.46 (s, 4H), 4.73 (s, 1H), 6.88–6.92 (t, *J* = 8.8 Hz, 2H), 7.24–7.27 (d, *J* = 10.8 Hz, 2H), 9.33 (s, 1H). ¹³C NMR (100 MHz, DMSO-d₆): δ 27.29, 29.26, 31.22, 32.20, 50.73, 111.94, 126.07, 127.80, 127.87, 147.17, 149.30, 149.60, 194.46. Anal. calc. for C₂₃H₂₆FNO; C 75.18, H 7.13, N 3.81, O 8.71; found: C 75.13, H 7.18, N 3.78, O 8.76.

9-(4-Chlorophenyl)-3,3,6,6-tetramethyl-3,4,6,7,9,10-hexahydroacridine-1,8(2H,5H)-dione (8f). Mp: 295–297 °C; FT-IR (KBr, cm⁻¹) ν: 3288, 3205, 3068, 2956, 2869, 1643, 1608, 1475, 1363, 1223, 1171. ¹H NMR (500 MHz, DMSO): δ 0.91 (s, 6H), 1.04 (s, 6H), 2.08–2.11 (d, *J* = 16, 2H), 2.26–2.29 (d, *J* = 16, 2H), 2.50–2.60 (dd, *J* = 14.65, 4H), 4.51 (s, 1H), 7.18–7.20 (d, *J* = 8.2 Hz, 2H), 7.28–7.29
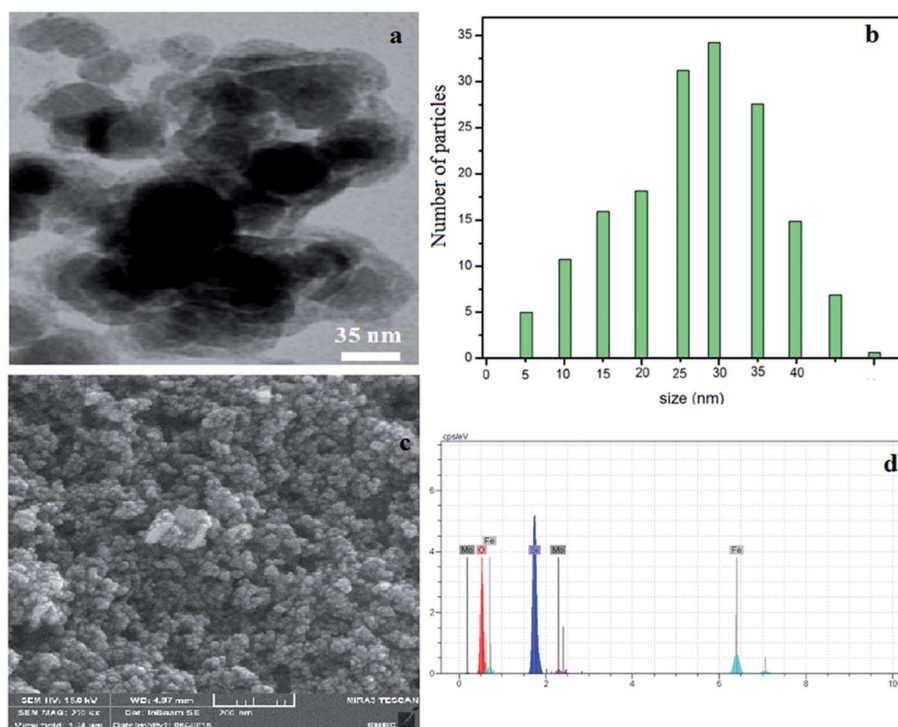

Fig. 3 TEM image of Fe₃O₄@SiO₂–MoO₃H (a), histogram of particle size distribution (b), SEM image of Fe₃O₄@SiO₂–MoO₃H (c) and EDAX spectrum of Fe₃O₄@SiO₂–MoO₃H (d).
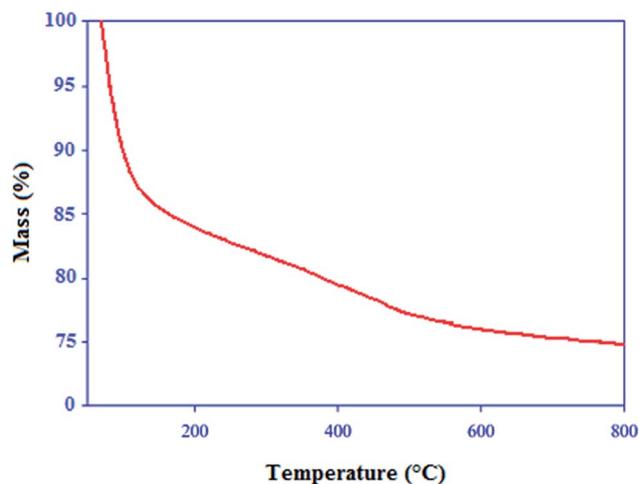
Fig. 4 TGA curve of $Fe_3O_4@SiO_2-MoO_3H$.

(d, J = 8.2 Hz, 2H), 9.32 (s, 1H). Anal. calc. for $C_{23}H_{26}ClNO_2$; C 71.96, H 6.83, N 3.65, O 8.33; found: C 71.90, H 6.89, N 3.59, O 8.32.

9-(4-Bromophenyl)-3,3,6,6-tetramethyl-3,4,6,7,9,10-hexahydro-acridine-1,8(2H,5H)-dione (8h). Mp: 310–312 °C; FT-IR (KBr, cm^{-1}) v: 3274, 3176, 3058, 2954, 2921, 1649, 1608, 1491, 1364, 1221, 1171. ^1H NMR (400 MHz, DMSO): δ 1.03 (s, 6H), 1.23 (s, 6H), 2.24–2.30 (dd, J = 14.8, 8.8 Hz, 4H), 2.44 (s, 4H), 4.84 (s, 1H), 7.16 (d, J = 6.8 Hz, 2H), 7.43 (d, J = 17.6 Hz, 2H), 9.30 (s, 1H). Anal. calc. for $C_{23}H_{26}BrNO_2$; C 64.49, H 6.12, N 3.27, O 7.47; found: C 64.52, H 6.17, N 3.31, O 7.49.

3,3,6,6-Tetramethyl-9-(4-nitrophenyl)-3,4,6,7,9,10-hexahydro-acridine-1,8(2H,5H)-dione (8i). Mp: 287–289 °C; FT-IR (KBr, cm^{-1}) v: 3384, 2958, 2908, 1643, 1602, 1514, 1447, 1364, 1221, 1171. ^1H NMR (500 MHz, DMSO): δ 0.91 (s, 6H), 1.05 (s, 6H), 2.08–2.11 (d, J = 6.5 Hz, 2H), 2.27–2.30 (d, J = 6.5 Hz, 2H), 2.50–2.63 (m, 4H), 4.63 (s, 1H), 7.45–7.48 (m, 2H), 8.10–8.12 (m, 2H),

9.32 (s, 1H). Anal. calc. for $C_{23}H_{26}N_2O_4$; C 70.03, H 6.64, N 7.10, O 16.22; found: C 70.08, H 6.69, N 7.07, O 16.26.

3,3,6,6-Tetramethyl-9-(3-nitrophenyl)-3,4,6,7,9,10-hexahydro-acridine-1,8(2H,5H)-dione (8j). Mp: 290–292 °C; FT-IR (KBr, cm^{-1}) v: 3282, 3193, 3070, 2957, 2930, 2889, 2870, 1649, 1612, 1577, 1434, 1364, 1225, 1171. ^1H NMR (500 MHz, DMSO): δ 0.91 (s, 6H), 1.05 (s, 6H), 2.09–2.12 (d, J = 4.4 Hz, 2H), 2.27–2.30 (d, J = 6.4 Hz, 2H), 2.55–2.63 (dd, J = 7.2 Hz, 4H), 4.64 (s, 1H), 7.55–7.58 (t, J = 3.1 Hz, 1H), 7.65–7.67 (d, J = 3 Hz, 1H), 7.99–8.02 (d, J = 5.1 Hz, 2H), 9.31 (s, 1H). Anal. calc. for $C_{23}H_{26}N_2O_4$; C 70.03, H 6.64, N 7.10, O 16.22; found: C 70.06, H 6.70, N 7.08, O 16.24.

3,3,6,6-Tetramethyl-9-(naphthalen-2-yl)-3,4,6,7,9,10-hexahy-droacridine-1,8(2H,5H)-dione (8k). Mp: 264–266 °C; IR (KBr, cm^{-1}) v: 3274, 3176, 3059, 2954, 2922, 1649, 1608, 1491, 1364, 1221, 1171. ^1H NMR (400 MHz, DMSO): δ 0.99 (s, 6H), 1.12 (s, 6H), 2.13–2.18 (d, J = 18 Hz, 2H), 2.21–2.23 (d, J = 9.6 Hz, 2H), 2.52 (s, 4H), 4.92 (s, 1H), 7.34–7.38 (d, J = 16, 1H), 7.46–7.47 (d, J = 6.8 Hz, 2H), 7.73–7.79 (m, 4H), 9.12 (s, 1H). Anal. calc. for $C_{27}H_{29}NO_2$; C 81.17, H 7.32, N 3.51, O 8.01; found: C 81.22, H 7.35, N 3.54, O 8.08.

Results and discussion

The MNPs **1** were prepared *via* a chemical co-precipitation[30] and were subsequently coated with a layer of silica using the sol–gel method[31] to provide reaction sites for further functionalization and thermal stability. The $Fe_3O_4@SiO_2$ nanoparticles **2** were then transformed to $Fe_3O_4@SiO_2-Cl$ with thionyl chloride and $Fe_3O_4@SiO_2-Cl$ were then transformed to $Fe_3O_4@SiO_2-OMoO_3H$ **3** *via* a nucleophilic substitution with anhydrous sodium molybdate in *n*-hexane to afford a dark gray powder (Scheme 1). We used acid–base potentiometric titration to measure the acid capacities of this catalyst. To this account, 100 mg of the catalyst was added to 10 ml of a 1 M NaCl solution and stirred continuously for 24 h at room temperature. The
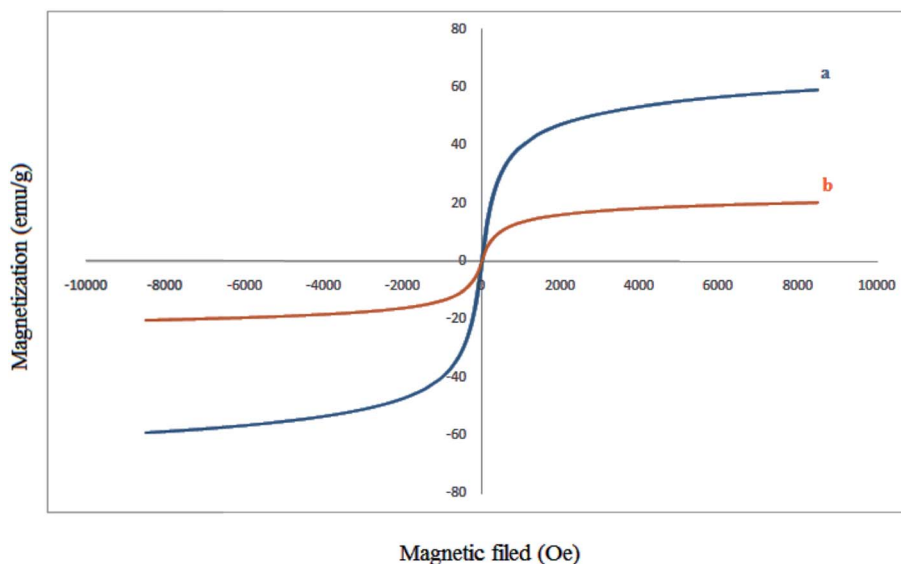

Fig. 5 Magnetization curves for the prepared Fe_3O_4 MNPs (a) and $Fe_3O_4@SiO_2-MoO_3H$ (b).

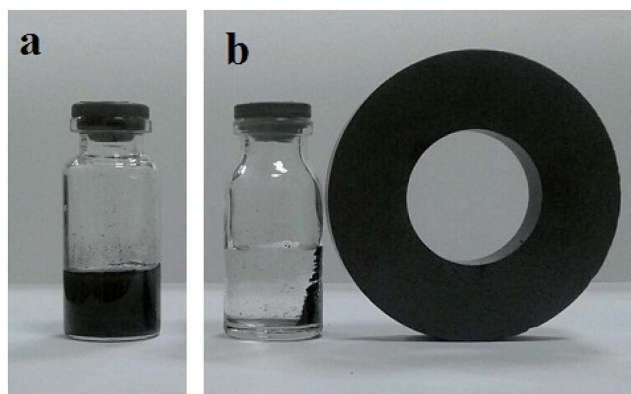**Fig. 6** Digital camera images of the aqueous solution with dispersed magnetic $Fe_3O_4@SiO_2-MoO_3H$ composite particles (a) and after applied magnetic field (b).

catalyst was separated using an external magnet, and the NaCl solution was decanted and saved. According to the obtained results, loading of acid sites was about 3.80 mmol H^+ per g of catalyst. The resulting MNP acid catalyst was characterized by XRD, FT-IR, ICP-OES, TEM, SEM and EDX. The percentage of molybdenum (Mo) in catalyst was also determined by ICP-OES at 8000–10 000 K which showed 1.68 (% w/w) molybdenum.

FT-IR spectra of catalyst are presented the band in the region of 560 cm^{-1} is attributed to the stretching vibrations of the (Fe–O) bond and the band at about 1090 cm^{-1} belongs to (Si–O) stretching vibrations. FT-IR analysis was used to characterize the presence of the $-MoO_3H$ groups on the surface of the MNPs (Fig. 1). As shown in Fig. 1c, the FT-IR spectra of $Fe_3O_4@SiO_2-MoO_3H$ was clearly different from those of Fe_3O_4 (Fig. 1a) and $Fe_3O_4@SiO_2$ (Fig. 1b). The broad peak in range of 1080–1200

cm^{-1} (attributed to the overlapping of peaks corresponding to Si–O–Si, Fe–O–Si, and symmetric MoO_2 stretching) indicated that the MNPs possessed MoO_3H groups.

The crystalline structure of the different synthesized materials was investigated by XRD. For the Fe_3O_4 particles (Fig. 2a), the diffraction peaks at $2\theta = 30.1°$, 35.4°, 43.1°, 53.6°, 57°, and 62.8° corresponded to the spinel structure of Fe_3O_4, which can be assigned to the diffraction of the (220), (311), (400), (422), (511), and (440) planes of the crystals, respectively.[32] For the $Fe_3O_4@SiO_2-OMoO_3H$ (Fig. 2b), the XRD pattern indicated that the crystalline structure of the Fe_3O_4 particles was retained after the deposition of SiO_2 layers. The broad peak at around $2\theta = 20°$ to 27° indicated the presence of amorphous silica in $Fe_3O_4@SiO_2-OMoO_3H$. The intensity of this peak increased with the introducing of molybdate on the silica-coated magnetic nanoparticles, which can be attributed to the amorphous molybdate supported on the composite. The XRD results showed that the $Fe_3O_4@SiO_2$ particles have been successfully coated with molybdate.

The TEM image revealed that the $Fe_3O_4@SiO_2-MoO_3H$ nanoparticles were uniform with an average size in the range of 10–30 nm (Fig. 3a).

The SEM image shown in (Fig. 3c) demonstrates that $Fe_3O_4@SiO_2-MoO_3H$ nanoparticles are nearly spherical with more than 20 nm in size.

The successful incorporation of molybdate groups was also confirmed by EDAX analysis (Fig. 3d), which showed the presence of to Fe, Si, Mo and O elements.

The thermogravimetric analysis (TGA) was used to study the thermal stability of the acid catalyst (Fig. 4). The first weight loss which occurred below 150 °C, displayed a mass loss that was attributable to the loss of adsorbed solvent or trapped water from the catalyst. A weight loss of approximately 5% weight
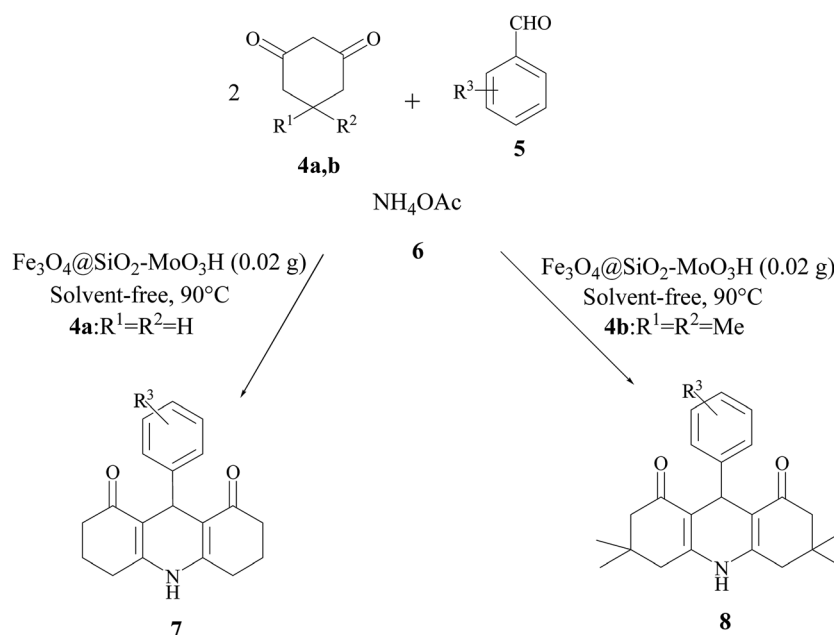
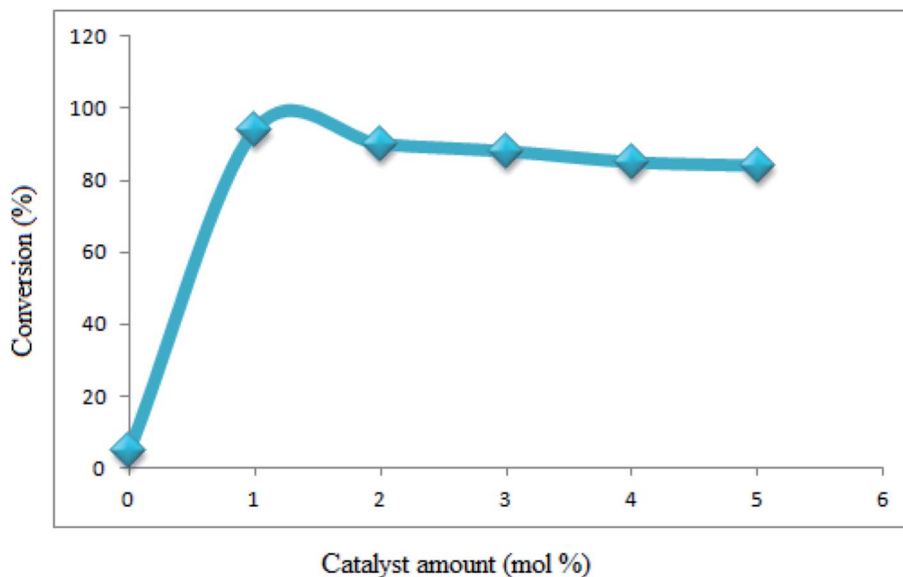**Scheme 2** Synthesis of 1,8-dioxo-decahydroacridine derivatives by $Fe_3O_4@SiO_2-MoO_3H$.

Fig. 7 Optimization of the catalyst amount.

Table 1 Optimization of model reaction by using various solvents and amount of $Fe_3O_4@SiO_2-MoO_3H$

Entry	Catalyst (mol%)	Solvent	Time (min)	Isolated yield (%)
1	1	EtOH	80	50
2	2	EtOH	80	45
3	3	EtOH	80	35
4	1	MeOH	80	55
5	1	CHCl$_3$	100	30
6	1	Toluene	140	20
7	1	DMF	220	25
8	1	Solvent-free	35	93
9	2	Solvent-free	35	90
10	3	Solvent-free	35	88

occurred between 300 and 500 °C which can be attributed to the loss of molybdate groups covalently bound to silica surface. Thus, it can be concluded that the catalyst is stable up to 300 °C.

Typical magnetization curve for Fe_3O_4 nanoparticles and $Fe_3O_4@SiO_2-MoO_3H$ are shown in Fig. 5. Room temperature specific magnetization (M) *versus* applied magnetic field (H) curve measurements of the sample indicate a saturation magnetization value (M_s) of 20.30 emu g^{-1}, lower than that of bare MNPs (59.14 emu g^{-1}) due to the coated shell.

Fig. 6a shows the photograph of $Fe_3O_4@SiO_2-MoO_3H$ microspheres that dispersed in water. After a magnet was placed aside, the black microspheres can be magnetized in 3 min, leaving a clear solution (Fig. 6b). That is to say, the

Table 2 Preparation of 1,8-dioxo-decahydroacridine derivatives using $Fe_3O_4@SiO_2-MoO_3H$

Entry	R^1=R^2	R^3	Product	Time (min)	Isolated yield (%)	Melting point (°C)
1	H	H	**7a**	35	93	278–279
2	H	4-Cl	**7b**	20	89	295–297
3	H	4-Br	**7c**	25	91	311–312
4	H	4-CH$_3$	**7d**	45	88	254–255
5	H	4-OH	**7e**	55	86	303–305
6	H	4-OCH$_3$	**7f**	50	86	302–304
7	H	3-NO$_2$	**7g**	25	90	280–282
8	CH$_3$	H	**8a**	25	92	291–293
9	CH$_3$	4-OCH$_3$	**8b**	40	90	275–277
10	CH$_3$	4-OH	**8c**	45	88	302–304
11	CH$_3$	4-CH$_3$	**8d**	55	90	267–269
12	CH$_3$	4-F	**8e**	30	94	289–291
13	CH$_3$	4-Cl	**8f**	20	92	295–297
14	CH$_3$	2-Cl	**8g**	20	90	222–224
15	CH$_3$	4-Br	**8h**	25	91	310–312
16	CH$_3$	4-NO$_2$	**8i**	35	93	287–289
17	CH$_3$	3-NO$_2$	**8j**	30	91	290–292
18	CH$_3$	2-Naphthaldehyde	**8k**	45	86	264–266
19	CH$_3$	4-(CH$_3$)$_2$–N	**8l**	50	88	217–219
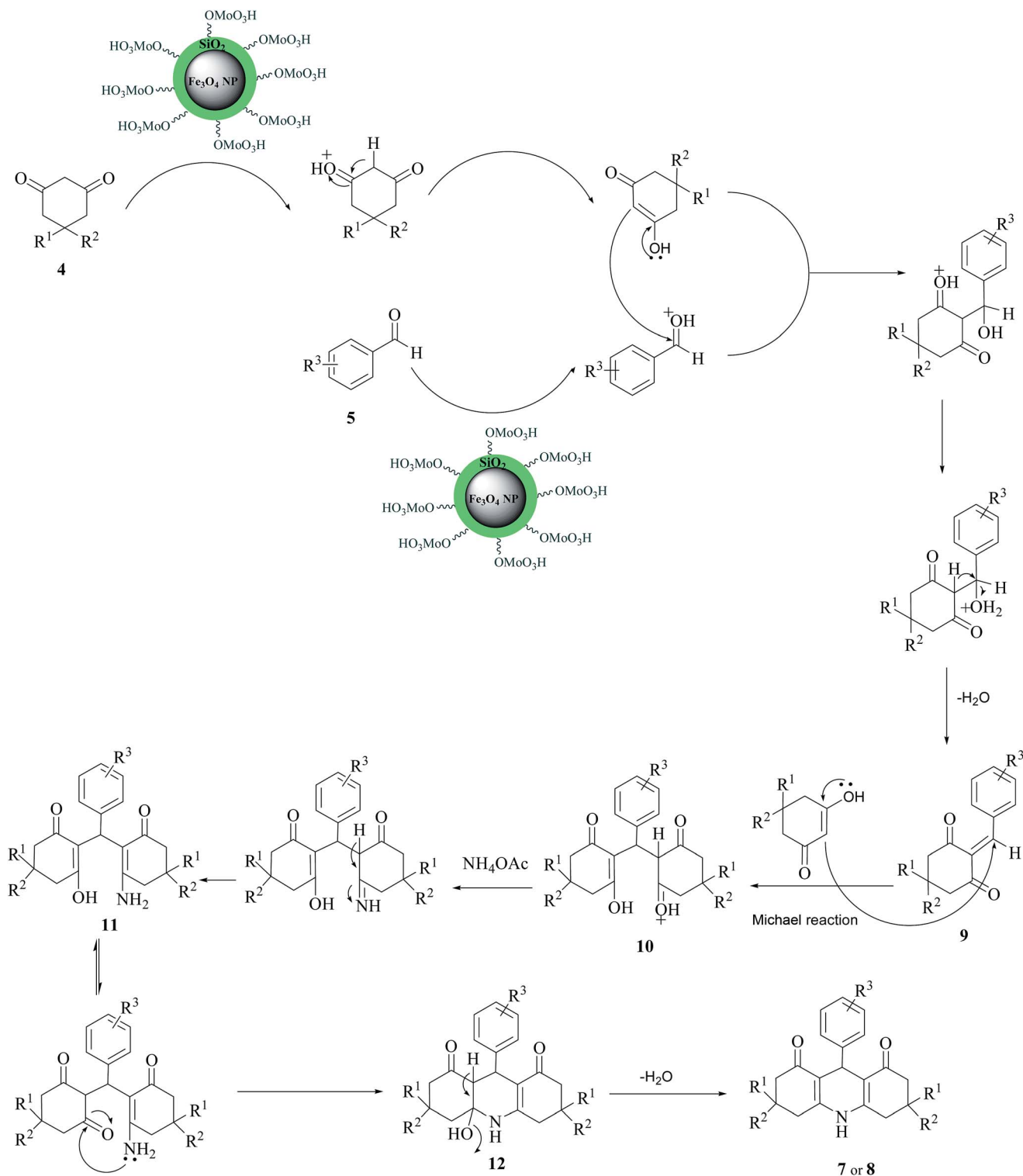
Scheme 3 Reasonable mechanism for the formation of decahydroacridine-1,8-diones.

$Fe_3O_4@SiO_2–MoO_3H$ nanoparticles were shown good magnetic responsibility even if the $SiO_2–MoO_3H$ layer was increased to 20 nm.

In continuation of our interest in the development of novel, efficient, and green procedures for the synthesis of organic compounds using safe catalysts,[33–35] we decided to prepare 1,8-

dioxo-decahydroacridines **7,8** was obtained was synthesized by condensation between dimedone (**4**) (2 mmol), benzaldehyde (**5**) (1 mmol) and ammonium acetate (**6**) (1 mmol) under solvent-free conditions as a model reaction (Scheme 2).

The reaction conditions were optimized on the basis of the catalyst, solvent and different temperature for the synthesis of
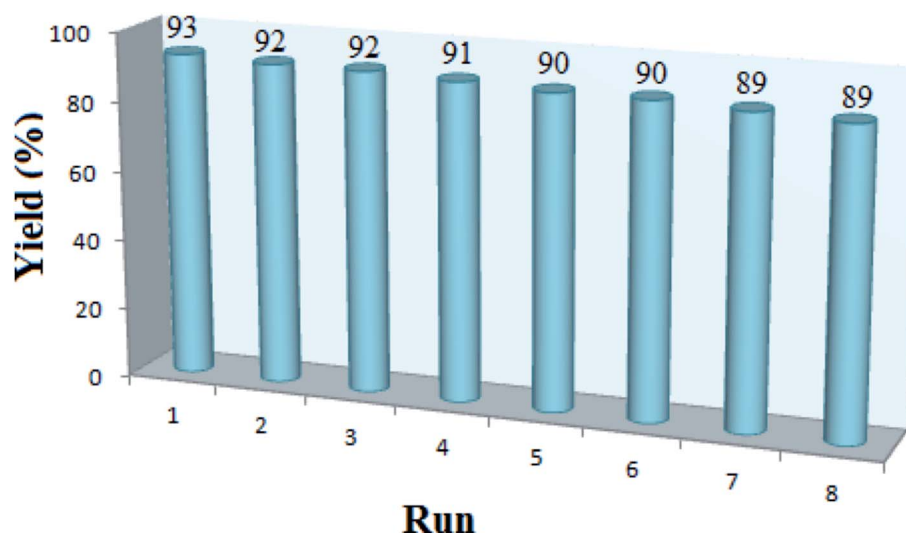
Fig. 8 Reusability of $Fe_3O_4@SiO_2-MoO_3H$ for synthesis of **7a**.

1,8-dioxo-decahydroacridines. This reaction was firstly examined in the absence of catalyst which did not show any appreciable progress even after 360 min. Upon screening, the results well showed that the reaction proceeds efficiently by adding 1 mol% of $Fe_3O_4@SiO_2-MoO_3H$. Also, increasing the catalyst amount did not improve the results (Fig. 7).

Eventually to making sure that the solvent free condition is appropriate, it has been decided to investigate the effect of different classical solvents such as EtOH, MeOH, $CHCl_3$, toluene, and DMF (Table 1, entries 1–7). We found that polar and protic solvents, such as EtOH or MeOH, afford better yields than aprotic ones. As it is shown in Table 1, using these solvents gave significantly lower yields and longer reaction times. Increasing the reaction times did not improve the yields. So the best yield of product was provided in solvent free conditions (Table 1, entry 8).

After optimization of the reaction conditions, in order to extend the scope of this reaction, a wide range of aromatic aldehydes were used with **4** and **6** (Table 2). All the products were characterized by comparison of their spectra and physical data with those reported in the literature.[36,37]

As indicated in Table 2, the new conditions are very suitable for a vast variety of aromatic aldehydes with both electron-donating and electron-withdrawing groups to give corresponding 1,8-dioxo-decahydroacridine derivatives in good to excellent yields. In all cases, the reactions proceeded within 20–55 minute. However, it is notable that substituted aromatic aldehydes with electron-withdrawing groups increase the rate of reaction (Table 2, entries 2, 3, 7, 12–17) probably by activating the carbonyl group as electrophile center. Contrarily in the case of electron-donating groups, the reaction was more slowly (Table 2, entries 4–6 and 9–11).

The reaction mechanism is shown in Scheme 3. At first, the acid catalyst changes the aldehyde into convenient electrophile *via* protonation of the carbonyl group and then one molecule of dimedone condenses with the aromatic aldehyde to produce intermediate **9**. Then the active methylene group of the second

molecule of dimedone reacts with **9** to give intermediate **10**. Nucleophilic attack of amine group of ammonium acetate to carbonyl group creates intermediate **11**. In the next step, cyclization will occur by the nucleophilic attack of amine group to carbonyl group to obtain intermediate **12**. Finally, by the removal of one water molecule, the acridine derivatives **7** or **8** will be generated.

The design and synthesis of recoverable catalysts is a highly challenging interdisciplinary field, which combines chemistry, materials science, and engineering from economic and environmental perspective. The main disadvantage for many of the reported methods is that the catalysts are destroyed in the work-up procedure and cannot be recovered or reused. In this process, as outlined in Fig. 8, the recycled catalyst can be used in up to eight cycles, during which there are negligible losses in the catalytic activity. The percentage of molybdenum (Mo) in recovered catalyst was also determined by ICP-OES at 8000–10 000 K which showed 1.67 (% w/w) molybdenum. Additionally the acid capacity of catalyst was 3.7 mmol H^+ per g after eighth recovery which confirms excellent efficiency of the immobilization of acidic group on the surface of the catalyst.
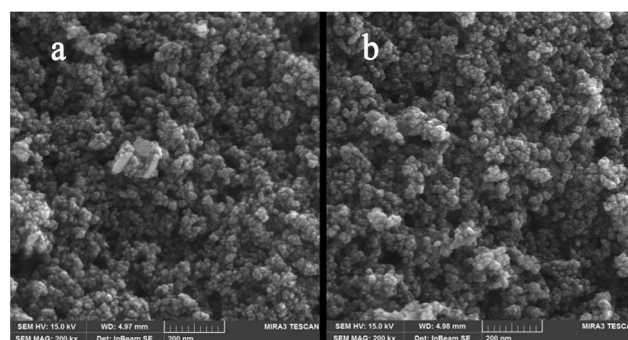

Fig. 9 FE-SEM images of (a) fresh $Fe_3O_4@SiO_2-MoO_3H$, (b) after reused eight times.

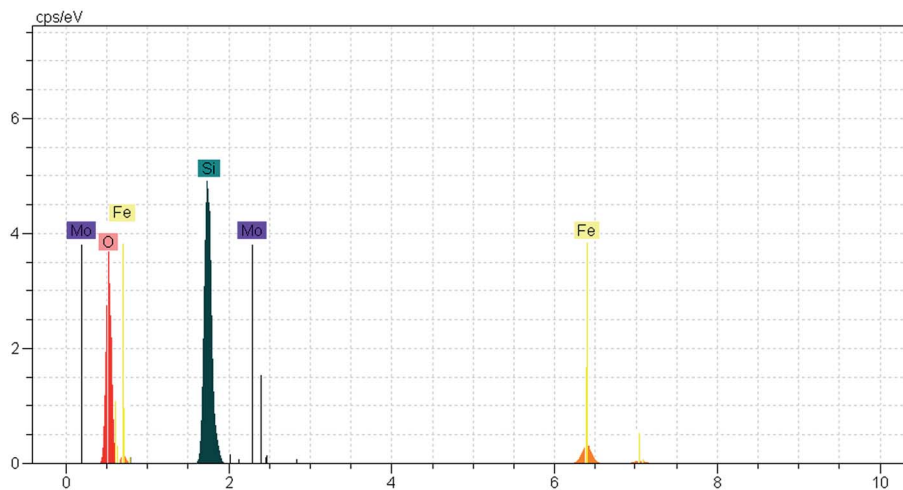**Fig. 10** EDAX spectrum of $Fe_3O_4@SiO_2$–MoO_3H after reused eight times.

After the eight recycles, the recovered catalyst had similar morphology as the fresh one (Fig. 9) and no noticeable change in structure was observed, by reference to the EDAX analysis as compared to the fresh catalyst (Fig. 10).

Conclusions

In summary, we found $Fe_3O_4@SiO_2$–$OMoO_3H$ as an effective and environmentally safe acidic magnetic catalyst which successfully catalyzed to produce 1,8-dioxo-decahydroacridines from aromatic aldehydes, an amine and a dimedone under solvent free conditions. By this development, the scope of heterocyclic compounds was increased. High catalytic activity under solvent free conditions, high yields, a clean process, reusable several times without loss of activity or selectivity simple catalyst preparation, easy separation after the reaction by a magnet and green conditions are advantages of these protocols.

Acknowledgements

Notes and references

1 B. Zhang, H. Asakura, J. Zhang, J. Zhang, S. De and N. Yan, *Angew. Chem., Int. Ed.*, 2016, **55**, 8319–8323.

2 E. L. S. Ngee, Y. Gao, X. Chen, T. M. Lee, Z. Hu, D. Zhao and N. Yan, *Ind. Eng. Chem. Res.*, 2014, **53**, 14225–14233.

3 Y. Wang, S. De and N. Yan, *Chem. Commun.*, 2016, **52**, 6210–6224.

4 H. L. Ding, Y. X. Zhang, S. Wang, J. M. Xu, S. C. Xu and G. H. Li, *Chem. Mater.*, 2012, **24**, 4572–4580.

5 J. Zou, Y. G. Peng and Y. Y. Tang, *RSC Adv.*, 2014, **4**, 9693–9700.

6 R. Zhao, K. Jia, J. J. Wei, J. X. Pu and X. B. Liu, *Mater. Lett.*, 2010, **64**, 457–459.

7 J. Liu, R. Che, H. Chen, F. Zhang, F. Xia, Q. Wu and M. Wang, *Small*, 2012, **8**, 1214–1221.

8 Y. Piao, A. Burns, J. Kim, U. Wiesner and T. Hyeon, *Adv. Funct. Mater.*, 2008, **18**, 3745–3758.

9 C. Wang, J. Yan, X. Cui and H. Wang, *J. Colloid Interface Sci.*, 2011, **354**, 94–99.

10 H. D. Oh and S. W. Lee, *Mater. Res. Bull.*, 2013, **48**, 2191–2193.

11 M. A. Ghasemzadeh, J. Safaei-Ghomi and H. Molaei, *C. R. Chim.*, 2012, **15**, 969–974.

12 Y. Mikata, M. Yokoyama, K. Mogami, M. Kato, I. Okura, M. Chikira and S. Yano, *Inorg. Chim. Acta*, 1998, **279**, 51–57.

13 I. Antonini, P. Polucci, L. R. Kelland, E. Menta, N. Pescalli and S. Martelli, *J. Med. Chem.*, 1999, **42**, 2535–2541.

14 M. J. Wainwright, *J. Antimicrob. Chemother.*, 2001, **47**, 1–13.

15 L. Ngadi, A. M. Galy, J. P. Galy, J. Barbe, A. Cremieux, J. Chevalier and D. Sharples, *Eur. J. Med. Chem.*, 1990, **25**, 67–70.

16 S. A. Gamega, J. A. Spicer, G. J. Atwell, G. J. Finlay, B. C. Baguley and W. A. Deny, *J. Med. Chem.*, 1999, **42**, 2383–2393.

17 S. Gallo, S. Atifi, A. Mohamoud, C. Santelli-Rouvier, K. Wolfart, J. Molnar and J. Barbe, *Eur. J. Med. Chem.*, 2003, **38**, 19–26.

18 K. Venkatesan, S. S. Pujari and K. V. Srinivasan, *Synth. Commun.*, 2009, **39**, 228–241.

19 X. S. Wang, D. Q. Shi, D. Q. Zhang, Y. F. Wang and S. J. Tu, *Chin. J. Org. Chem.*, 2004, **24**, 430–432.

20 W. Shen, L. M. Wang, H. Tian, J. Tang and J. J. Yu, *J. Fluorine Chem.*, 2009, **130**, 522–527.

21 M. Dabiri, M. Baghbanzadeh and E. Arzroomchilar, *Catal. Commun.*, 2008, **9**, 939–942.

22 M. Kidwai and D. Bhatnagar, *Tetrahedron Lett.*, 2010, **51**, 2700–2703.

23 F. Rashedian, D. Saberib and K. Niknam, *J. Chin. Chem. Soc.*, 2010, **57**, 998–1006.

24 B. Das, P. Thirupathi, I. Mahender, V. S. Reddy and Y. Koteswara, *J. Mol. Catal. A: Chem.*, 2006, **247**, 233.

25 A. Davoodnia, A. Khojastehnezhad and N. Tavakoli-Hoseini, *Bull. Korean Chem. Soc.*, 2011, **32**, 2243.

26 T. S. Jin, J. S. Zhang, T. T. Guo, A. Q. Wang and T. S. Li, *Synthesis*, 2004, **12**, 2001–2005.

27 B. Karami and M. Kiani, *Catal. Commun.*, 2011, **14**, 62–67.

28 B. Karami, M. Kiani, S. J. Hosseini and M. Bahrami, *New J. Chem.*, 2015, **39**, 8576–8581.

29 B. Karami and M. Kiani, *Res. Chem. Intermed.*, 2016, **42**, 3373–3383.

30 A. Bee, R. Massart and S. J. Neveu, *J. Magn. Magn. Mater.*, 1995, **149**, 6–9.

31 R. V. Ferreira, I. L. S. Pereira, L. C. D. Cavalcante, L. F. Gamarra, S. M. Carneiro, E. J. Amaro, J. D. Fabris, R. Z. Domingues and A. L. Andrade, *Hyperfine Interact.*, 2010, **195**, 265–274.

32 L. Cabrera, S. Gutierrez, M. P. Morales, N. Menendez and P. Herrasti, *J. Magn. Magn. Mater.*, 2009, **321**, 2115–2120.

33 B. Karami and M. Kiani, *J. Chin. Chem. Soc.*, 2015, **62**, 756–765.

34 B. Karami and M. Kiani, *J. Iran. Chem. Soc.*, 2016, **13**, 111–116.

35 B. Karami, M. Kiani and M. A. Hoseini, *Chin. J. Catal.*, 2014, **35**, 1206–1211.

36 G. M. Ziarani, A. Badiei, M. Hassanzadeh and S. Mousavi, *Arabian J. Chem.*, 2014, **7**, 335–339.

37 M. Nasr-Esfahani and T. Abdizadeh, *C. R. Chim.*, 2015, **18**, 547–553.